Supplementary appendix

Deep phenotyping unaffected *BMPR2* mutation carriers in the screening for pulmonary arterial hypertension

E.N. Toth*[1,2], L.R. Celant*[1,2], M. Niglas[5], S.M.A. Jansen[1,2], J. Tramper [1,2] ,N. Baxan[5], A. Ashek[5] , J.N. Wessels [1,2], J.T. Marcus[2,3], L.J. Meijboom[2,3],A.C. Houweling[4], E.J. Nossent[1], J. Aman[1], J. Grynblat[6] , F. Perros[7] , D. Montani [8,9,10], A. Vonk Noordegraaf[1,2],Lan Zhao[5], F.S. de Man[2] , and H.J. Bogaard[1,2]

*Contributed equally

Affiliations

[1]Amsterdam UMC location Vrije Universiteit Amsterdam, Department of Pulmonary Medicine, De Boelelaan 1117, Amsterdam, the Netherlands

[2]Amsterdam Cardiovascular Sciences, Pulmonary Hypertension and Thrombosis, Amsterdam, the Netherlands

[3]Amsterdam UMC location Vrije Universiteit Amsterdam, Department of Radiology and Nuclear Medicine, De Boelelaan 1117, Amsterdam, the Netherlands

[4] Amsterdam UMC location AMC, Department of Genetics, Meibergdreef 9, Amsterdam, the Netherlands

[5] Imperial College London, National Heart and Lung Institute, Du Cane Road, London W12 0NN, UK

[6] INSERM UMR_S 999, Hôpital Marie Lannelongue Le Plessis Robinson France, Université Paris Saclay, Congenital and Pediatric Cardiology Department, APHP, Université Paris Cité, Necker-Enfants Malades Hospital.

[7] CarMeN Laboratory, INSERM U1060, INRAE U1397, Université Claude Bernard Lyon 1, Pierre-Bénite, France

[8] Universite Paris-Saclay, School of Medicine Gif-sur-Yvette, Île-de-France, France

[9] Hopital Bicetre, Service de Pneumologie et Soins Intensifs Respiratoires Le Kremlin-Bicetre, Île-de-France, France

[10] INSERM UMRS 959, Hôpital Marie Lannelongue Paris, Île-de-France, France

Supplementary Methods

Transgenic Bmpr2$^{\Delta 71Ex1/+}$ Rat Model

Haemodynamic measurements

At the endpoint, the rats were anaesthetized (2.7 ml/kg i.p. of Hypnorm: Hypnovel : H2O = 1:1:2), right ventricular systolic pressure (RVSP) and pulmonary arterial pressure (PAP) were measured via a pre-curved catheter inserted through the right jugular vein and systemic blood pressure (SBP) recorded in the carotid artery cannulation using a PowerLab Data Acquisition system (ADInstruments Ltd). Following sacrifice, hearts were dissected and fixed with 10% formalin in phosphate-buffered saline and processed for histological examination with Pirco-Sirius red staining (fibrosis), as well as double immunofluorescence staining with CD31 (1/100; Abcam) and Alexa Flour 488 conjugated wheat germ agglutinin (WGA; 1/1000; ThermoFisher; green) for assessment of capillary density and cardiomyocytes hypertrophy.

Cardiac magnetic resonance imaging (cMRI)

cMRI images were obtained in the Biological Imaging Centre at Imperial College London on a 9.4T Bruker scanner (Bruker BioSpec, Ettlingen, Germany). The rats were anaesthetised with isoflurane (5%) and kept/adjusted to maintain a respiratory rate of around 40 - 60 breaths per minute during the CMR. Heart rate was monitored by ECG throughout the cMRI examination. Body temperature was monitored and kept at around 37 °C using a heating mat. All cMRI acquisitions were prospectively triggered with the ECG R-wave and breathing rate. A T1-weighted gradient echo fast low angle shot (FLASH) sequence was used to acquire 2D multi-slice stack of images. The following parameters were used: repetition time (TR) was RR interval/number of frames (~ 6.2 ms for ~ 27 frames); echo time (TE) 2.3 ms; effective repetition time was the RR interval; flip angle was 18o; scan time ≤18min. CINE image in-plane spatial resolution was (200 x 200) µm2 with a slice thickness of < 1.5 mm. Interslice thickness adjustments were made on a subject basis to

cover both ventricles as well as to capture the following anatomical landmarks – the apex and base of the RV, the aortic valve and the top of LV wall.

The end-diastolic and end-systolic images were segmented manually by two experienced observers via a free open-source software ITK-Snap for evaluation of cardiac indices characterising cardiac phenotypes. Stroke volume (SV) was defined as the difference between ED volume (EDV) and ES volume (ESV); SV = EDV – ESV. Cardiac output (CO) was derived from the following calculation: CO = HR * SV / 1000, units are ml/min. The EF was defined as EF = SV / EDV * 100%. Mass was calculated by multiplying the specific myocardial density (1.05 g /ml) with the ED myocardial volume. This was calculated with the Meeh's formula205 – BSA = k * W2/3 / 10000, where k is a constant 9.83 and W is body weight in grams, resulting BSA is in cm2. The RV to PA coupling was determined by the ratio of RV ESV over RV SV206, a cMRI-based surrogate marker for ventricular-arterial coupling.

DOLPHIN-GENESIS: Baseline and follow-up assessment of unaffected carriers of a pathogenic BMPR2 variant and healthy controls

Genetic testing of potential participants

Patients in whom a pathogenic variant was identified were provided with a family letter, containing information about the identified genetic predisposition for PAH, general information on the disease, the heritability, and the option informing their close relatives about genetic testing. In addition, a form was provided to the general practitioner for referral to the outpatient clinic of clinical genetics. Relatives who wished to undergo genetic testing were tested for the familiail pathogenic variant after receiving genetic counseling. 27 genes were examined (*ABCC8* (NM_001351295.2), *ACVRL1* (NM_000020.3), *AQP1* (NM_198098.4), *ATP13A3* (NM_001367549.1), *BMP10* (NM_014482.3), *BMPR1A* (NM_004329.3), *BMPR1B* (NM_001256793.2), *BMPR2* (NM_001204.7), *CAV1* (NM_001753.5), *EIF2AK4* (NM_001013703.4), ENG (NM_001114753.3), *FBLN2* (NM_001998.3), *FOXF1* (NM_001451.3), *GDF2* (NM_016204.4), *GGCX*

(NM_000821.7), *KCNK3* (NM_002246.3), *KDR* (NM_002253.4), *KLF2* (NM_016270.4), *KLK1* (NM_002257.4), *NOTCH3* (NM_000435.3), *PDGFD* (NM_033135.4), *SMAD1* (NM_005900.3), *SMAD4* (NM_005359.6), *SMAD9* (NM_001127217.3), *SOX17* (NM_022454.4), *TBX4* (NM_018488.3), *TET2* (NM_001127208.3)). Additional multiplex ligation-dependent Probe Amplification (MLPA) was used on *BMPR2* to ensure deletions or duplications were not missed.

Cardiac Magnetic Resonance Imaging (cMRI) image acquisition

All cMRI imaging was performed on a Siemens 1.5T Avanto or Sonato scanner (Siemens, Medical Solutions, Erlangen, Germany), equipped with a six-element phased-array receiver coil. Image acquisition, volume, and mass measurements were performed using the methodology previously described in the van der Veerdonk et al. [1]. All cMRI imaging was assessed by two independent observers using Circle (Circle cvi42 release 5.12.4 Circle Cardiovascular Imaging, Calgary, Canada). All indexed parameters were matched to the body surface area.

Strain

cMRI feature tracking was applied to detect quantitative motion changes of the RV and LV throughout the cardiac cycle. The endo- and epi-cardial border surfaces of both ventricles were manually delineated, and the automated tracking algorithm was applied. Tracking performance was visually reviewed to ensure accuracy. Longitudinal strain was measured using the same feature tracking technology applied to the 4-chamber view. In case of insufficient border tracking, manual adjustments were made to the initial contour and the algorithm was reapplied.

PA flow

Phase contrast velocity encoded images were made with prospective ECG-gating during a single breath hold. Image orientation was orthogonal to the main pulmonary artery. The pulmonary vessel contour was manually traced in a single phase to demarcate a region of interest and tracked in all phases using automatic contour detection. Peak velocity and maximum/minimum pulmonary artery area were automatically calculated from the contoured area. The region of interest was manually controlled and, if necessary, corrected in every phase. Presence of pulmonary artery flow notching was visually scored. PA flow was quantified using the methods described by Rolf et al. [2]. Acceleration time and ejection time were determined based on automatically generated flow time curves.

Cardiopulmonary Exercise Testing (CPET)

CPET was performed and using the methodology previously described by Groepenhoff et al.[3]. During exercise testing, participants were monitored using electrocardiogram (ECG). All CPET data was reviewed by an experienced pulmonologist in accordance with ESC/ERS guidelines (source).

Transthoracic Echocardiography (TTE)

Echocardiography was performed using a PHILIPS Sparq Ultrasound System (Amsterdam, the Netherlands) previously described by Spruijt et al. [4].

Right Heart Catheterization

A 7-F balloon tipped, flow-directed Swan-Ganz catheter (131HF7, Baxter, Healthcare Corp Irvine, California) was inserted via the jugular vein under local anesthesia and brought into position. Participants were

continuously monitored with the use of electrocardiography. Hemodynamic parameters were assessed in resting condition as described previously in van de Veerdonk et al.[5]

Pressure volume loops

Pressure volume analysis in unaffected mutation carriers was performed manually by the investigators[6]. Derivation of RV end-systolic elastance (Ees) was done via the single beat method[7], using mPAP to estimate end systolic pressure[8]. Arterial elastance (Ea) and end-diastolic elastance (Eed) were derived as described previously[9]. Beats with significant catheter artefacts were excluded.

Supplementary tables

Supplementary table S1. Overview of pathogenic *BMPR2* variants in the DOLPHIN-GENESIS cohort

ID	Family ID	Nucleotide change	Amino Acid Change	ACMG classification
1	A	c.1454A>G[¥]	p.(Asp485Gly)	Pathogenic
2	A	c.1454A>G	p.(Asp485Gly)	Pathogenic
3	A	c.1454A>G	p.(Asp485Gly)	Pathogenic
4	A	c.1454A>G	p.(Asp485Gly)	Pathogenic
5	A	c.1454A>G	p.(Asp485Gly)	Pathogenic
6	A	c.1454A>G	p.(Asp485Gly)	Pathogenic
7	A	c.1454A>G	p.(Asp485Gly)	Pathogenic
8	A	c.1454A>G	p.(Asp485Gly)	Pathogenic
9	A	c.1454A>G	p.(Asp485Gly)	Pathogenic
10	B	c.1454A>G	p.(Asp485Gly)	Pathogenic
11	B	c.1454A>G	p.(Asp485Gly)	Pathogenic
12	B	c.1454A>G	p.(Asp485Gly)	Pathogenic
13	C	c.(1276+1_1277-1)_(1413+1_1414-1)	Del exon 10	Pathogenic
14	C	c.(1276+1_1277-1)_(1413+1_1414-1)	Del exon 10	Pathogenic
15	D	c.(1276+1_1277-1)_(*1_?)	Del exon 10-13	Pathogenic
16	E	c.1978G>T[¥]	p.(Glu660*)	Pathogenic
17	E	c.1978G>T	p.(Glu660*)	Pathogenic
18	F	c.277G>T	p.(Glu93*)	Pathogenic
19	F	c.277G>T	p.(Glu93*)	Pathogenic
20	G	c.1525G>T	p.(Glu509*)	Pathogenic
21	H	c.619dup	p.(Glu207Glyfs*13)	Pathogenic
22	I	c.637C>T	p.(Arg213*)	Pathogenic
23	J	c.200A>G	p.(Tyr67Cys)	Pathogenic
24	K	c.399delT -> c.399del	p.(Pro133fsLeufs*18)	Pathogenic
25	K	c.399del	p.(Pro133fsLeufs*18)	Pathogenic
26	L	c.2752C>T	p.(Gln918*)	Pathogenic
27	M	c.168del	p.(Thr57fGlnfs*21)	Pathogenic

28	N	c.248-2A>G	p.(?)	Pathogenic

[¥]Indicates pathogenic variant identified in participants who developed pulmonary arterial hypertension throughout the study. * Indicates a stop codon.

Supplementary table S2. Linear regression analyses of right - ventricular volumes, mass and global circumferential strain.

RVEDVi mL/m²				
Coefficients	**Estimate**	**Standard error**	**t-value**	***p-value***
Gender	-13.4955	3.7983	-3.553	0.000629***
Age	-0.5059	0.1130	-4.477	5.71e-05 ***
BMPR2 carrier	-14.2180	3.8473	-3.696	0.000629***
RVESVi mL/m²				
Coefficients	**Estimate**	**Standard error**	**t-value**	***p-value***
Gender	-7.71288	2.16357	-3.565	0.000924***
Age	-0.28998	0.06438	-4.504	5.23e-05 ***
BMPR2 carrier	-5.59387	2.19150	-2.553	0.014419*
RV GCS (%)				
Coefficients	**Estimate**	**Standard error**	**t-value**	***p-value***
Gender	-1.01911	0.67740	-1.504	0.14030
Age	-0.07002	0.2006	-3.491	0.001167**
BMPR2 carrier	-2.88786	0.68167	-4.236	0.000125***
RV mass				
Coefficients	**Estimate**	**Standard error**	**t-value**	***p-value***
Gender	-1.75471	1.41853	-1.237	0.2230
Age	-0.08406	0.04221	-1.991	0.05330
BMPR2 carrier	-2.91836	1.43684	-2.031	0.0486*

RVEDVi: indexed right ventricular end diastolic volume; BMPR2; bone morphogenetic protein receptor type 2; RVESVi: indexed right ventricular end systolic volume; RV GCS: right ventricular global circumferential strain; RV: right ventricular.

Supplementary table S3. Haemodynamic measurements from the right ventricular catheterisation procedure from wild type (WT) and *Bmpr2* transgenic (*Bmpr2*$^{\Delta 71Ex1/+}$) rats.

Haemodynamic measurements	Wild type	*Bmpr2*$^{\Delta 71Ex1/+}$
BW (g)	506 ± 45.4	494 ± 30.0
HR (bpm)	299 ± 43.6	279 ± 61.2
mPAP (mmHg)	17.5 ± 1.76	16.7 ± 2.89
PADP (mmHg)	11.6 ± 1.33	10.7 ± 3.14
PASP (mmHg)	25.6 ± 2.69	24.3 ± 2.85
RVSP (mmHg)	33.5 ± 2.11	27.8 ± 5.33
RVEDP (mmHg)	11.1 ± 15.1	4.63 ± 11.2
Min dP/dt (mmHg/s)	-1333 ± 278.5	-1123 ± 240.8
Max dP/dt (mmHg/s)	1269 ± 174.1	1024 ± 195.4
Contractility index (1/s)	77.7 ± 33.9	61.9 ± 12.4

Data are presented as mean ± standard deviation.

BW: body weight; HR: heart rate; mPAP: mean pulmonary artery pressure; PADP: pulmonary artery diastolic pressure; PASP: pulmonary artery systolic pressure; RVSP: right ventricular systolic pressure; RVEDP: right ventricular end diastolic pressure; dP/dt max: maximal rate of pressure development; dP/dt min; maximal rate of pressure decay.

Supplementary table S4. Cardiac indices from cine scans of rats from wild type and *Bmpr2*$^{\Delta 71Ex1/+}$ rats.

Indices	Control n=5	*Bmpr2*$^{\Delta 71Ex1/+}$ n=6
BW (g)	465 ± 41.9	475 ± 20.4
HR (bpm)	332 ± 39.3	334 ± 31.3
RVEDVI (µl/cm^2)	1.29 ± 0.06	1.18 ± 0.06 *
RVESVI (µl/cm^2)	0.53 ± 0.05	0.51 ± 0.04
RVSVI (µl/cm^2)	0.75 ± 0.06	0.67 ± 0.05 *
RVCI (µl/min/m^2)	0.25 ± 0.02	0.22 ± 0.03
RVEF (%)	58.6 ± 3.54	57.1 ± 2.60
RVSV/RVESV	1.55 ± 0.21	1.34 ± 0.15
RVMI (mg/cm^2)	0.49 ± 0.04	0.44 ± 0.02 *
LVEDVI (µl/cm^2)	1.40 ± 0.14	1.27 ± 0.04 *
LVESVI (µl/cm^2)	0.54 ± 0.07	0.52 ± 0.04
LVSVI (µl/cm^2)	0.86 ± 0.08	0.74 ± 0.06 *
LVCI (µl/min/m^2)	0.29 ± 0.04	0.25 ± 0.03
LVEF (%)	61.4 ± 1.56	58.6 ± 3.67
LVSV/LVESV	1.59 ± 0.15	1.42 ± 0.22
LVMI (mg/cm^2)	1.11 ± 0.08	1.02 ± 0.06
VMI	0.44 ± 0.03	0.43 ± 0.02

Data are presented as mean ± standard deviation. Significance values were as follows: comparison to wild type * p<0.05, ** p<0.01, *** p<0.001.

BW: body weight; HR: heart rate; RVEDVi: indexed right ventricular end diastolic volume index; RVESVi: indexed right ventricular end systolic volume; RVSVi: indexed right ventricular stroke volume; RVCi: right ventricular cardiac index; RVEF: right ventricular ejection fraction; RVMi; indexed right ventricular mass; LVEDVi: indexed left ventricular end diastolic volume; LVSVI: indexed left ventricular stroke volume; LVCi: left ventricular cardiac index; LVEF: left ventricular ejection fraction; LVMi: indexed left ventricular mass; VMi: ventricular mass index.

Supplementary table S5. Comparison of baseline characteristics of unaffected carriers of a pathogenic *BMPR2* variant (DOLPHIN-GENESIS cohort) and the two subjects who developed pulmonary arterial hypertension (PAH) in the duration of the study.

	***BMPR2* carriers (n=26)**	***Conversion 1***	***Conversion 2***
Female (%)	16 (61.5)	Male	Male
Age	43.42 (16.23)	58	53
Serum NT-proBNP ($ng \cdot L^{-1}$)	22.53 (14.67)	24	4
Cardiopulmonary exercise testing			
VO2 max (mL/min)	2056.19 (601.54)	2553	NA
RER max	1.18 (0.06)	1.18	NA
PETCO2 max (kpa)	4.54 (0.81)	4.84	3.82
PETCO2 rest (kpa)	4.26 (0.42)	4.31	4.43
V'E/V'CO2 rest	33.36 (5.20)	35.1	31.1
V'E/V'CO2 max	32.82 (6.24)	34.4	37.4
V'E/V'CO2 AT	27.48 (3.44)	29.8	29.1
Max O2 pulse (mL/beat)	12.52 (3.38)	17.7	17.3
Echocardiography			
TRV ($m \cdot s^{-1}$)	2.15 (0.21)	NA	NA
TI (%)	6 (24)	None	None
RV hypertrophy (%)	0 (0.0)	None	None
Septal bulging (%)	0 (0.0)	None	None
PAAT ($cm \cdot s^{-1}$)	134.30 (16.73)	120	100
PASP (mmHg)	19.67 (5.03)	NA	NA
TAPSE (mm)	23.27 (2.87)	26	26
RV S' wave ($cm \cdot s^{-1}$)	11.91 (1.70)	14.6	12.9
Cardiac Magnetic Resonance Imaging			
RAi min (mL/ m^2)	15.36 (6.61)	19.14	29.19
RAi max (mL/ m^2)	28.66 (9.96)	34.66	52.15
LAi min (mL/ m^2)	11.22 (3.46)	6.22	8.13
LAi max (mL/ m^2)	29.84 (6.18)	19.15	23.44
RVEF (%)	57.13 (6.29)	55.45	55.00
RVEDVi (mL/ m^2)	62.43 (15.58)	64.1	69.32
RVESVi (mL/ m^2)	26.90 (8.47)	28.6	31.00
LVEF %	68.69 (9.44)	79.00	70.00
LVEDVi (mL/ m^2)	58.55 (10.93)	54.00	56.41
LVESVi (mL/ m^2)	19.17 (7.39)	11.26	17.21
RV GCS (%)	-15.87 (2.65)	-18.65	-16.5
LV GCS (%)	-19.66 (2.17)	-21.82	-18.6
Right Heart Catheterization			
	***BMPR2* carriers (n= 20)**	**Conversion 1**	**Conversion 2**

Heart rate	72.55 (11.98)	87	61
mPAP (mmHg)	16.25 (2.22)	20	18
mRAP (mmHg)	5.70 (2.15)	5.0	6.0
CO (L/min)	5.54 (1.07)	6.92	5.1
CI (L·min ·m^2)	3.11 (0.63)	3.31	2.44
PVR (WU)	1.04 (0.45)	1.73	1.96
PCWP (mmHg)	10.65 (3.12)	8.0	8.0

Data are presented as mean ± standard deviation

NT-proBNP: N-terminal pro-B-type natriuretic peptide. Cardiopulmonary exercise testing - max O2 pulse: maximum oxygen pulse; PETCO2 max: maximum end-tidal carbon dioxide pressure; PETCO2 rest: resting end-tidal carbond dioxide pressure; RER max: maximum respiratory exchange ratio; V'E/V'CO2 AT: ventilation/carbon dioxide production at anaerobic threshold; V'E/V'CO2 max: ventilation/carbon dioxide production at maximum exercise; V'E/V'CO2 rest: ventilation/carbon dioxide production at rest; VO2 max: maximum oxygen consumption. Echocardiography – PAAT: pulmonary artery acceleration time; PASP: pulmonary artery systolic pressure; RV: right ventricular; S' wave: doppler velocity of the tricuspid annulus during systole; TAPSE: tricuspid annular plane systolic; TI: tricuspid insufficiency; TRV: tricuspid regurgitant velocity. Cardiac magnetic resonance imaging - LAi max: left atrium indexed maximum volume; LAi min: left atrium indexed minimum volume; LVEDVi: left ventricular end-diastolic volume indexed; LVEF: left ventricular ejection fraction; LVESVi: left ventricular end-systolic volume indexed. LV GCS: left ventricular global circumferential strain; RAi max: right atrium indexed maximum volume; RAi min: right atrium indexed minimum volume; RVEDVi: right ventricular end-diastolic volume indexed; RVEF: right ventricular ejection fraction; RVESVi: right ventricular end-systolic volume indexed; RV GCS: right ventricular global circumferential strain. Right heart catheterization – mPAP: mean pulmonary artery pressure; mRAP: mean right atrial pressure; CO: cardiac output; CI: cardiac index; PVR: pulmonary vascular resistance; PCWP: pulmonary capillary wedge pressure.

Supplementary figures

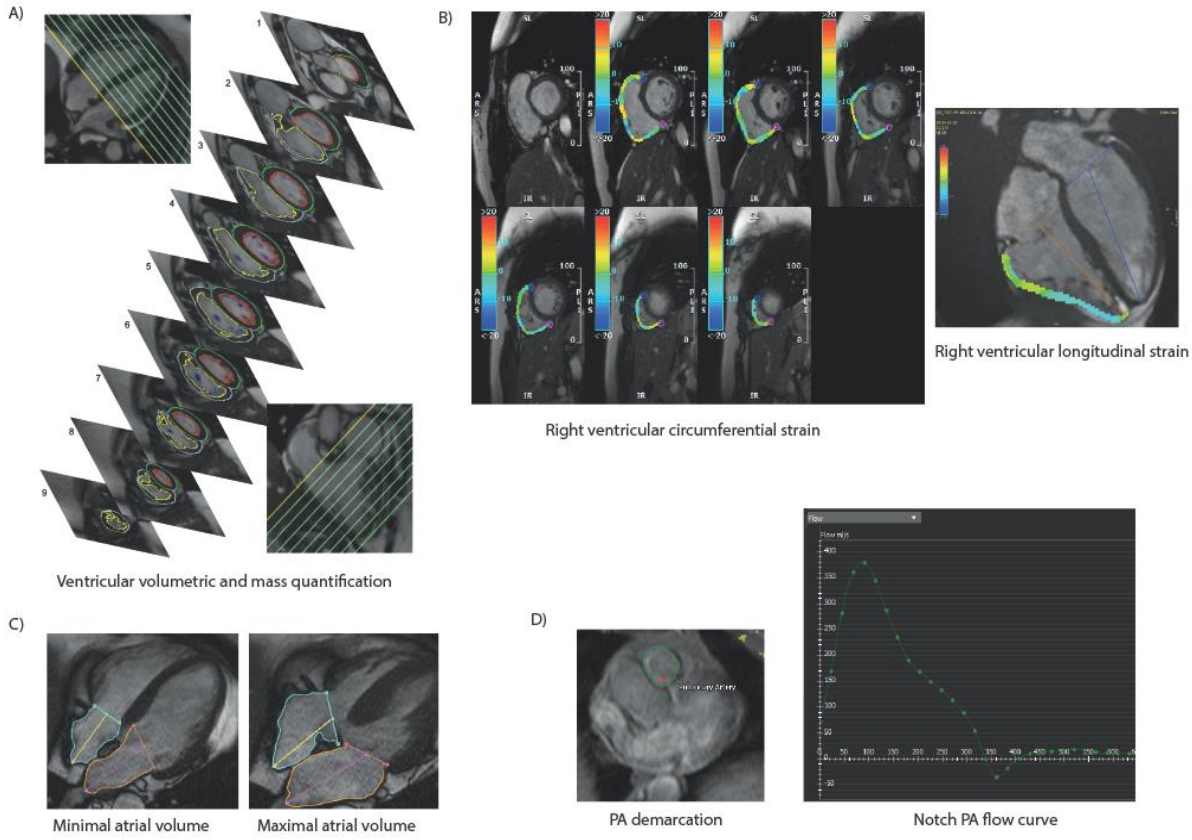

Supplementary figure S1. Description of cardiac magnetic resonance imaging methodology.

A. Ventricular and volumetric mass quantification. B. Left. Circumferential strain measurement. Right: longitudinal strain measurement. C. Atrial minimum and maximum volume. D. Left: PA flow measurement using vessel contouring and automatic phase tracking. Right: PA flow curve showing PA flow notching typically seen in pulmonary arterial hypertension.

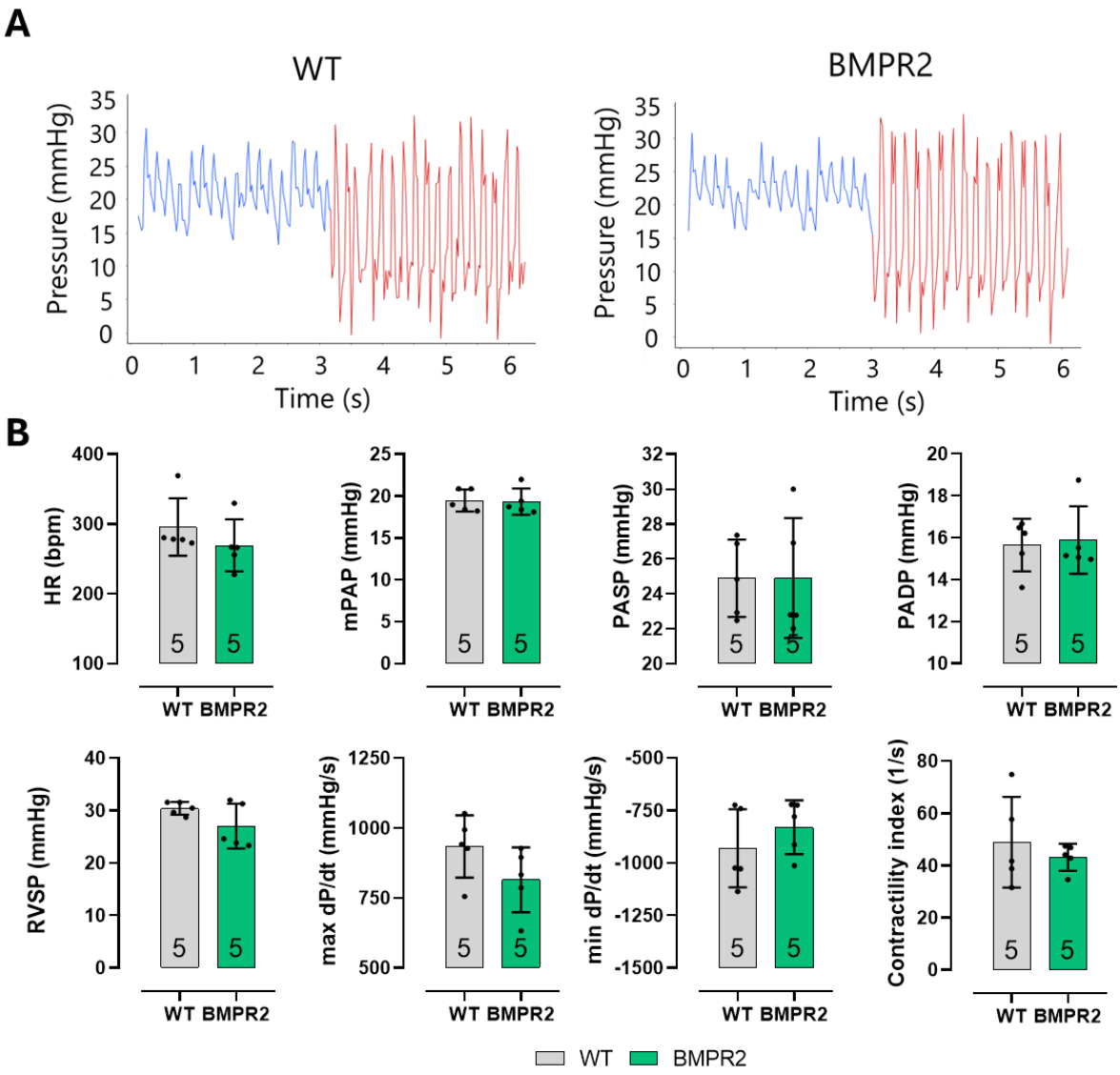

Supplementary figure S2. Haemodynamic measurements from male wild type (WT) and *Bmpr2* deficient (*Bmpr2*$^{\Delta 71Ex1/+}$) rats.

A. Right ventricular (RV) and pulmonary (PA) representative traces from WT (left) and *Bmpr2*$^{\Delta 71Ex1/+}$ (right) rats. B. Quantitative measurements of heart rate (HR), pulmonary arterial mean (mPAP), systolic (PASP) and diastolic (PADP) pressures, right ventricular systolic pressure (RVSP), maximum and minimum rate of rise of RV pressure (dP/dt), and contractility index (h). *N* numbers are displayed within each groups' bar in the graphs. Significance values were: * p<0.05; ** p<0.01, *** p<0.001 when compared to WT.

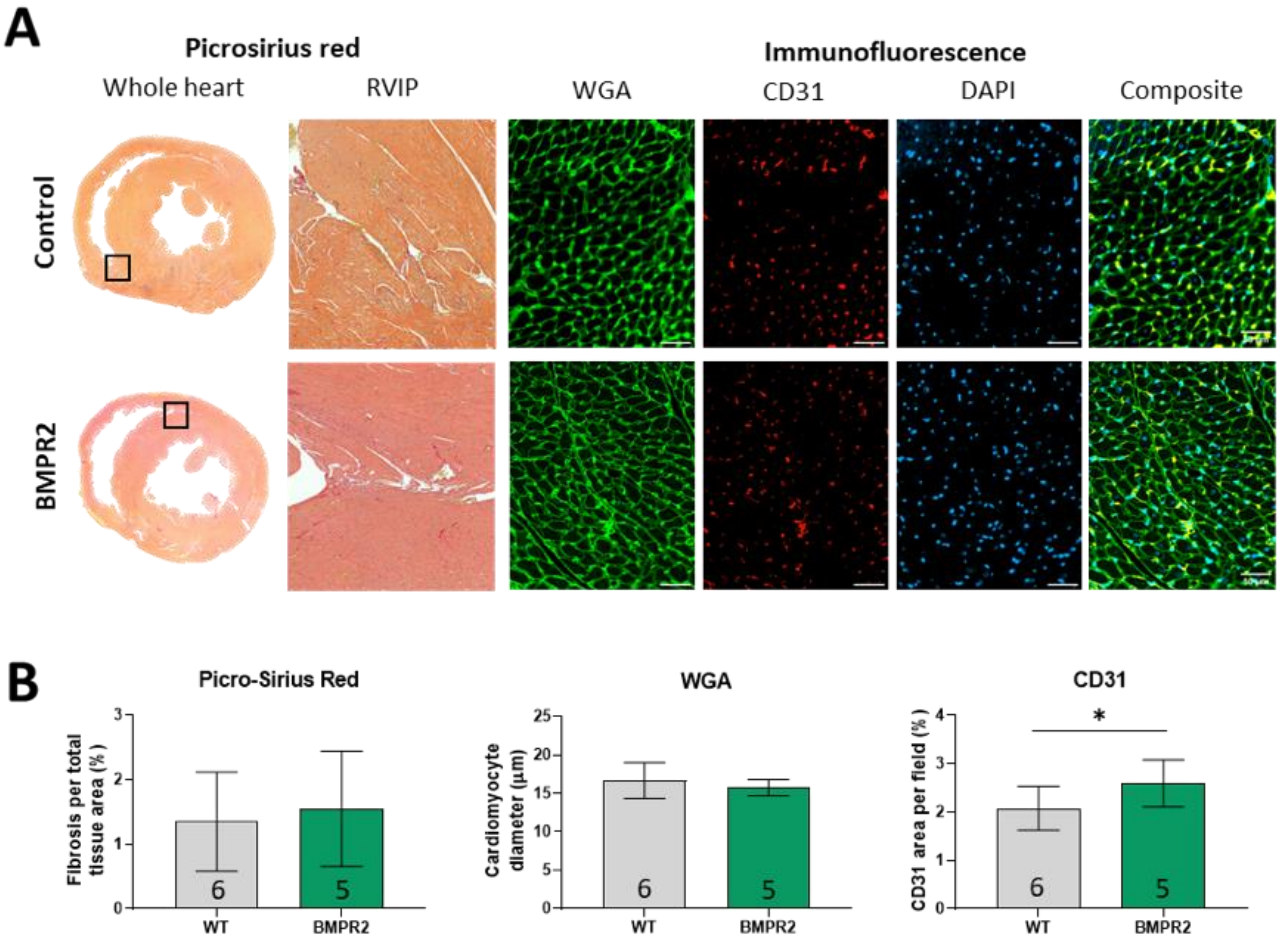

Supplementary figure S3. Representative wild-type (WT, n=6) and *Bmpr2* transgenic (*Bmpr2*$^{\Delta 71Ex1/+}$, n=5) rat cardiac histological images and corresponding image analysis.

A. Picrosirius red stained whole heart and right ventricular insertion points (RVIP) are displayed, along with double immunofluorescence images stained for cardiomyocyte periphery (WGA), endothelial cells (CD31) and nuclei (DAPI). The immunofluorescent stained images are also shown as a composite merged image. The length of the bar for fluorescence images is 50 µm; size of PCR-stained images is 1835 x 1655 µm. B. Picrosirius red staining over total tissue area, minimum cardiomyocyte from WGA staining, and CD31 staining as the total stained area to total tissue area were calculated. Significance values are as follows: * p<0.05; ** p<0.01, *** p<0.001. Significance values are as follows: * p<0.05; ** p<0.01, *** p<0.001.

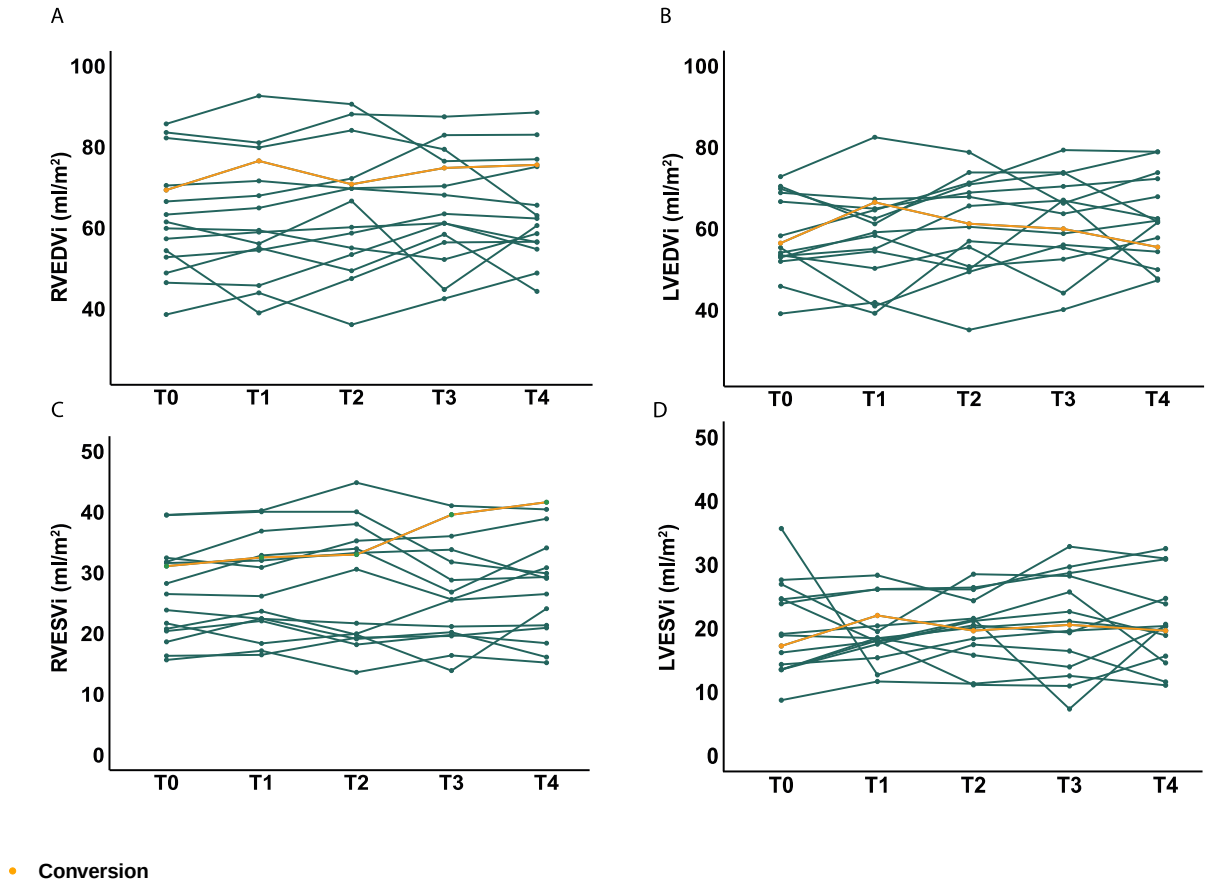

Supplementary figure S4. Longitudinal follow-up of unaffected carriers of a pathogenic BMPR2 variant.

A. Right ventricular end diastolic volume indexed (RVEDVi) over time. B. Right ventricular end systolic volume indexed (RVESVi) over time. C. Left ventricular end diastolic volume indexed (LVEDVi) over time. D. Left ventricular end systolic volume indexed (LVESVi) over time.

References

1. van de Veerdonk, M.C., et al., *The importance of trabecular hypertrophy in right ventricular adaptation to chronic pressure overload.* Int J Cardiovasc Imaging, 2014. **30**(2): p. 357-65.
2. Rolf, A., et al., *Pulmonary vascular remodeling before and after pulmonary endarterectomy in patients with chronic thromboembolic pulmonary hypertension: a cardiac magnetic resonance study.* Int J Cardiovasc Imaging, 2015. **31**(3): p. 613-9.
3. Groepenhoff, H., et al., *Prognostic relevance of changes in exercise test variables in pulmonary arterial hypertension.* PLoS One, 2013. **8**(9): p. e72013.
4. Spruijt, O.A., et al., *Serial assessment of right ventricular systolic function in patients with precapillary pulmonary hypertension using simple echocardiographic parameters: A comparison with cardiac magnetic resonance imaging.* J Cardiol, 2017. **69**(1): p. 182-188.
5. van de Veerdonk, M.C., et al., *Progressive right ventricular dysfunction in patients with pulmonary arterial hypertension responding to therapy.* J Am Coll Cardiol, 2011. **58**(24): p. 2511-9.
6. Trip, P., et al., *Clinical relevance of right ventricular diastolic stiffness in pulmonary hypertension.* Eur Respir J, 2015. **45**(6): p. 1603-12.
7. Trip, P., et al., *Accurate assessment of load-independent right ventricular systolic function in patients with pulmonary hypertension.* J Heart Lung Transplant, 2013. **32**(1): p. 50-5.
8. Tello, K., et al., *More on Single-Beat Estimation of Right Ventriculoarterial Coupling in Pulmonary Arterial Hypertension.* Am J Respir Crit Care Med, 2018. **198**(6): p. 816-818.
9. Wessels, J.N., et al., *Right atrial function is associated with right venticular diastolic stiffness: RA-RV interaction in pulmonary arterial hypertension.* Eur Respir J, 2022. **59**(6).